PRACTICALITIES OF RE-ENTRY PREDICTIONS – THE VEGA-01 AVUM CASE

B. Bastida Virgili [(1)], S. Lemmens [(2)], J. Siminski [(1)], Q. Funke[(1)]

[(1)] IMS Space Consultancy @ ESA Space Debris Office, ESOC/ESA, Robert-Bosch-Str. 5, 64293 Darmstadt, Germany
Email: benjamin.bastida.virgili@esa.int
[(2)] ESA Space Debris Office, ESOC/ESA, Robert-Bosch-Str. 5, 64293 Darmstadt, Germany

ABSTRACT

On the 2nd November 2016 the upper stage of the first VEGA launch re-entered into the Earth's atmosphere. The re-entry of this object was followed with special interest by ESA (as ESA is the launching state for this object), and also in an internationally coordinated re-entry test campaign of the Inter-Agency Space Debris Coordination Committee (IADC).

In this paper, we show the obtained prediction results using different orbit propagators and effective drag coefficient estimation methods. We also show the influence of the atmosphere models regarding the use of different solar activity proxies in the past, but also with different prediction values. These aspects are combined with the orbit measurement data fusion experiments that have been conducted to obtain accurate re-entry prediction results. ESA's main objective of the experiments is to further automate the process which currently requires some expert interaction to exploit its full capabilities.

1 INTRODUCTION

1.1 Re-entries at ESA

ESA has been hosting technical workshops on re-entries since the early 80's because ESA provides a re-entry service to ESA's member states and has also the responsibility for ESA-registered objects. The ESA Space Debris Office (SDO) is tasked with the related development and research, and provides the re-entry service to registered users.. In addition, ESA, as member of IADC, coordinates the re-entry campaigns of IADC (campaign administration, web-based front-end hosting and maintenance). Both functions are interlaced in this paper, as the re-entry object AVUM was under ESA responsibility, and it was selected as the test object for an IADC re-entry test campaign.

An automated re-entry predictions process was set at ESA in 1999, with the LASCO (Lifetime Assessment for Catalogued Objects) [1] tool, which computes in a fully automated way the remaining lifetime for all objects in the public TLE catalogue and generates re-entry predictions. The results are accessible for a limited number or people via the DISCOS (Database and Information System Characterizing Objects in Space) web interface [2]. Since 2013 the results of the LASCO analysis containing the re-entry predictions for the following two months are more proactively distributed via e-mail to stakeholders. Shortly after, in 2014, a new tool was created, called RAPID, which automatizes the call to separate existing tools that are used to generate more accurate predictions during the last month of a re-entry, and with the capability of additional plots generation. The last step on this modernisation was taken in 2016, with the setup of a two-tier web based data distribution [3] aimed at civil protection agencies, with some contribution for the general public as well as part of ESA's educational responsibility.

A more detailed explanation of the capabilities of the tools can be found in [4].

1.2 VEGA-01

The maiden flight of the VEGA rocket occurred from Guiana Space Center (Kourou) at 10:00 UTC of the 13th of February 2012. ESA took the legal responsibility of being the launching state for this maiden flight (as done in the past with other European launchers first flights). After a successful launch, the Vega's AVUM (Attitude & Vernier Upper Module) fourth stage first reached a circular orbit at an altitude of 1450 km and an inclination of 70º above the equator where it released LARES (Laser Relativity Satellite). It then manoeuvred to lower its perigee to 350 km before deploying the other satellites that it was carrying (ALMASat-1 of the University of Bologna and seven CubeSats from different universities of Europe, thanks to the support of the ESA's Education Office). The mission aimed at qualifying the overall Vega system, including the vehicle, the ground infrastructure and operations from the launch campaign to the payload separation and disposal of the upper module [5].

This final orbit was selected in order to make sure that the small satellites released, as well as the AVUM, would comply with the LEO mitigation guidelines requiring a de-orbit in less than 25 years after the end of the operational life (as proposed by IADC in 2002 [6] and adopted by ESA in 2009). All the CubeSats have already decayed; concretely between end of 2014 and beginning of 2015. ALMASat, according to ESA's

Proc. 7th European Conference on Space Debris, Darmstadt, Germany, 18–21 April 2017, published by the ESA Space Debris Office
Ed. T. Flohrer & F. Schmitz, (http://spacedebris2017.sdo.esoc.esa.int, June 2017)

predictions, will decay at the end of 2019. The exception is LARES which was injected in an orbit from where it would take millennia to decay.

The object of interest for this study, the upper stage, re-entered into the Earth's atmosphere on the 2nd November 2016. This VEGA AVUM upper stage (with international COSPAR designator 2012-006K, and with NORAD catalogue number #38086), had still attached the LARES-A&H/SS platform (Avionic & Harness / Support System). The upper stage has a shape defined by the combination of a cone and a disk shape with approximate dimensions 1.9 m in diameter by 2.1 m in height, and a launch mass of about 960 kg, as can be seen integrated before launch in Fig. 2.

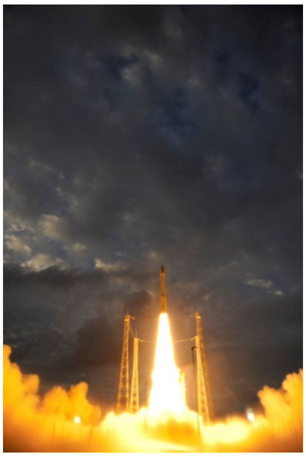

Figure 1.Picture of Vega-01 launch

Figure 2. AVUM with LARES-A&H/SS platform. ALMAsat and the Cubesats dispensers are also visible.

1.3 AVUM re-entry campaign

In April 2016, the Vega-01 AVUM was selected as candidate for an internationally coordinated re-entry test campaign of the Inter-Agency Space Debris Coordination Committee (IADC). Since then, at the ESA SDO the system was set up so that RAPID would run the more precise predictions for the AVUM once per day, using for each prediction the most recent 20 US TLE available at that time. The evolution of these predictions (including the uncertainty window) are shown in Fig. 3. Some large variations can be observed in these long term predictions, which are mainly due to the difference between the predicted and the observed solar activity (shown in Fig. 4).

The IADC test campaign opened on the 18th October 2016, two weeks before the predicted re-entry, when the object had approximately a perigee and apogee height of 199 km and 301 km, respectively, and 69.45 deg inclination. This opening marked the start of a period of intense manual calibration work.

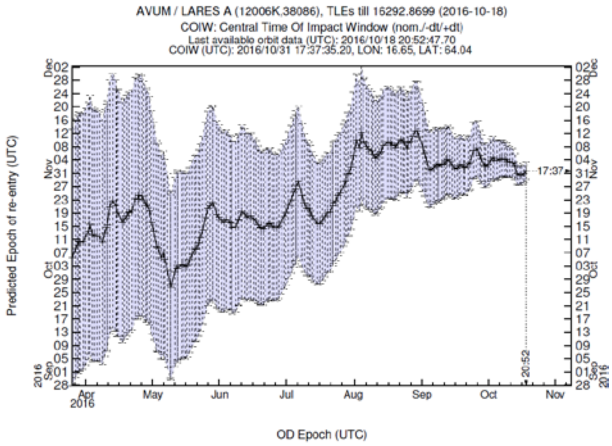

Figure 3. Automated re-entry predictions for the AVUM since April 2016.

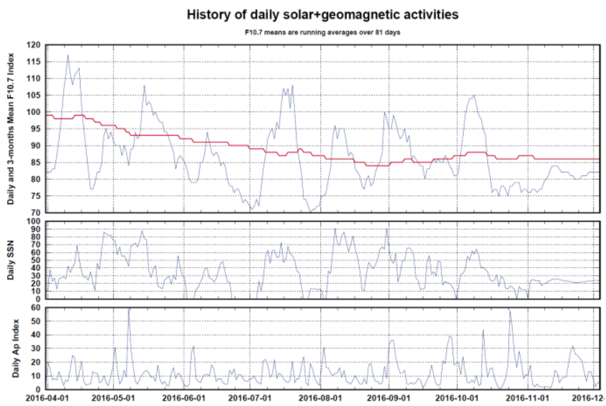

Figure 4. Solar and geomagnetic activity indices from April until December 2016.

2 PRACTICALITIES FOR THE RE-ENTRY OF VEGA-01

Since the opening of the IADC campaign, and until two days before the re-entry, ESA was issuing a daily prediction to civil protection agencies within ESA member states using all sources of information available. On the last 48 hours of the campaign, there was a constant monitoring of new data, and if the quality of the data was considered acceptable, predictions were provided every few hours.

There are several factors that make difficult to automatize a re-entry campaign and that are the cause of having large uncertainty windows (usually a 20% of the remaining time is considered). They are mainly related to the real behaviour of the atmosphere compared to what the models predict, which directly relates to the solar activity. Namely, the differences between the real and the predicted solar activity, and the handling of storm periods in the atmosphere models, have a major impact in the re-entry predictions. During the AVUM re-entry campaign, the observed solar activity was very unsettled, with two important solar storms, surrounded by rather calm periods.

Another factor influencing the re-entry prediction process is the orbital data used for the predictions. There may be many different sources of data, provided in different formats like TLEs, orbital state vectors, or ephemeris, and even sometimes also raw data from sensors. In that case, an additional process is needed to compute an orbit determination. In addition, on the last hours of a re-entry it seems to be more difficult to generate an accurate orbital state, causing the last inputs to the prediction process to be noisy. For the AVUM campaign, we received TLEs from international partners through the IADC exchange website for re-entry campaigns, TIRA radar tracks, EISCAT range measurements and we tried to obtain SLR (satellite laser ranging) data, without success due to bad meteorological conditions. In some cases, it was necessary to manually filter out data which is clearly wrong (in the sense that it does not match the previous data points for the predictions). In other cases, when data seems to be noisy but could be used, we performed a combination of noisy data in order to derive a mean state with less noise.

All these factors set challenges to any re-entry prediction process. Different ways to improve the process under such conditions could be analysed by ESA for this particular re-entry case.

2.1 Data sources

In the scope of an ESA study, laser ranging of the re-entering AVUM was attempted from few laser stations in central Europe. However, none of the attempts was successful because of bad weather conditions. This was a first test to track non-cooperative objects at such a low altitude and during the re-entry phase, when the prediction accuracy becomes bad. Therefore, it is also not sure that it would have worked with more favourable weather conditions.

2.1.1 TIRA

To generate ESA orbital states and provide TLEs to the IADC campaign, we contracted the FHR/TIRA of the Fraunhofer Research Establishment, located close to Bonn, in Germany, shown in Fig. 5. It consists of a tracking radar, working in L-Band (1.333 GHz), which also has imaging capabilities in Ku-Band (16.7GHz). As research organisation, tracks can mainly be obtained during working hours. Therefore, TIRA passes of the AVUM were taken on the 20th, 27th and 28th of October, being impossible to get a pass closer to the re-entry time due to weekend and official holidays. For the first two passes, separated a week, imaging was also taken in order to estimate the attitude of the object and possible changes (see Fig. 6). Both times the data provided similar results with respect to the attitude, with an estimated intrinsic rotation rate between 14°/s and 16°/s.

Figure 5. FHR/TIRA radar.

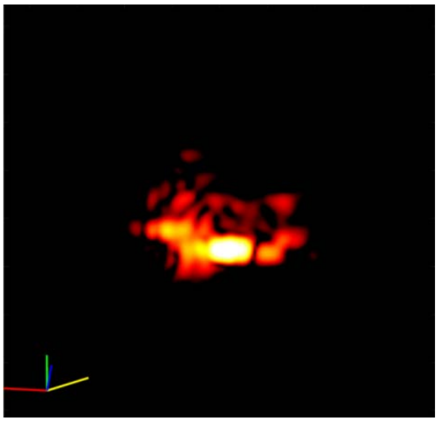

Figure 6. TIRA image of the AVUM on the 20th of October.

Based on the pass data provided by TIRA, we performed an orbit determination using the tool ODIN (Orbit Determination by Improved Normal Equations) [7]. For the three passes we were able to obtain nice residuals and a good fit, from which we generated a TLE to share with the IADC members. In the cases where we had only one pass available (in the 20th, for example), we simulated another pass based on TLE data in order to get a better Cd estimation. Ideally, 3 passes separated by around 24h and in different flight directions give an optimal combination to perform a very precise OD, but with 2 passes and enough spacing it is also possible. For this campaign, we shared the obtained TIRA data with our US colleagues operating the Space Surveillance Network, as part of the Data Sharing Agreement existing between ESA and JSpOC. and we got confirmation that the provided data could be incorporated in their orbit determination process.

2.1.2 EISCAT

EISCAT (European Incoherent SCATter Scientific Association) is an international scientific association with member institutes in several countries [8]. It conducts ionospheric and atmospheric measurements with radars. It operates in three countries: Finland, Norway and Sweden, and all facilities are located north of the Arctic circle.

Although they have a swamped scientific schedule, they were able to schedule observations with brief notice time for the AVUM re-entry. Even without having tracking capabilities, the EISCAT radar in Tromsoe (see Fig. 7) was able to acquire one pass on the 21st, two passes on the 22nd October and one on the 1st November (very close to the re-entry epoch), with short arcs (3 to 5 seconds). EISCAT performed the tracking as activity inside a SSA ESA project. The residuals obtained from the observations directly were small, providing confidence on the quality of the data (see Fig. 8).

Figure 7. EISCAT radar in Tromsoe.

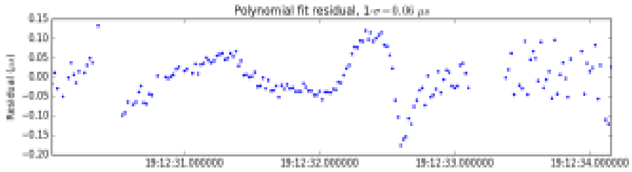

Figure 8. Round-trip delay residuals of pass of AVUM over EISCAT on 22nd of October

Even with the short arcs, the data from EISCAT could be used in the orbit determination process and helped to obtain an orbit for the AVUM which was more accurate than the TLEs, by using a combination of the passes on the 21st and 22nd. The data consisted on round-trip delay and Doppler shift, which could be converted to the internal used range and range-rate. The use of both types of measurements gave worse results that only using range, for which we have not yet determined a reason. As EISCAT is a scientific organisation and the tracking of debris is in testing phase, for all the passes the data was provided at least with one day of delay, and required a pre-processing. This means that for the last pass, on the 1st of November, the data could not be used in real time to fit an orbit. For this particular pass, however, EISCAT operators provided a very rapid confirmation on the observation of the object, with a delay of about 10 seconds to the expected passage time according to the most recent TLE.

2.2 Solar activity

ESA's Space Debris Office has its own solar and geomagnetic activity prediction model (SOLMAG) [9], which uses data from past solar cycles to predict the future ones. SOLMAG has a short term prediction algorithm (which covers with predicted daily values only the following solar rotation), and a medium and long term prediction algorithm (for the next centuries, with predicted values provided on a monthly basis). The medium and long-term prediction method implemented in SOLMAG is based on the regression technique of McNish and Lincoln [9], which is similar to that used by Holland and Vaughan [10].

The SOLMAG long term predictions were used for the forecasts for the re-entry of the AVUM since April 2016 (as shown in Fig. 3). This long term solar activity prediction is done only once per month, and then a single value is provided for a complete month. These are the main causes of the oscillations that can be observed in a re-entry prediction if done in a long term (more than one month ahead of the re-entry).

For the final part of a re-entry campaign, the short term predictions of SOLMAG are used, and then the variation on the re-entry forecast tends to be smaller. However, we have observed that in SOLMAG (and also in other solar activity prediction tools), solar storms tend to be under-predicted (as can be seen in Fig. 9), while the prediction of the solar flux are usually more accurate (as seen in Fig. 10). Furthermore, in SOLMAG only a daily Ap value is predicted, while in reality, the variations have a much shorter span, and with the observed data values every 3 hours are provided. It is possible to get better predictions for the very short term (up to three days), based on the expert assessment of the SIDC (Solar Influences Data Analysis Center), which is the solar physics research department of the Royal Observatory of Belgium [12]. These predictions have been incorporated to the SOLMAG process and may improve the re-entry predictions in the future. However, this functionality was not yet in place for the AVUM re-entry campaign, and although re-entry predictions were performed with a changed solar activity forecast, the results were not completely satisfactory and therefore, not stored.

As the re-entry predictions use the solar activity forecasts, if a storm was under-predicted and then in reality it had a larger effect, the time to re-entry would tend to get shortened. This happened few days before the opening of the AVUM re-entry campaign, when a storm on the 13th of October made the re-entry epoch jump back by 3 days. During the campaign itself, the observed solar activity was very unsettled, with two important solar storms on the 25th and on the 29th of October, and a rather calm period at the beginning, as can be seen in Fig. 11 and Fig. 12. These factors caused the predictions to oscillate a lot, more than in other re-entry campaigns. In order to compensate for the oscillations of the solar activity, the time span used for the drag coefficient computation was varied between 1.5 and 8 days, so that storms were taken or not into account, as well as calm periods.

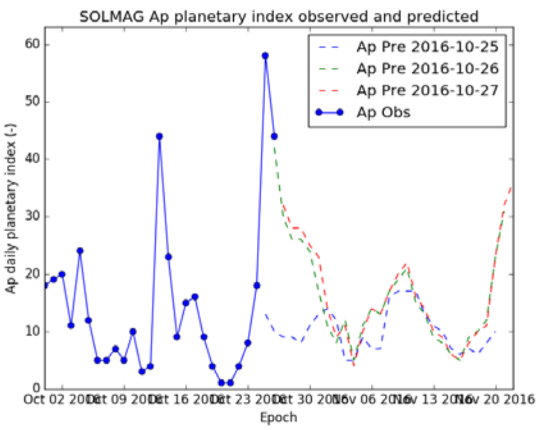

Figure 9. Observed Ap planetary index versus predicted flux at different epochs during the re-entry campaign.

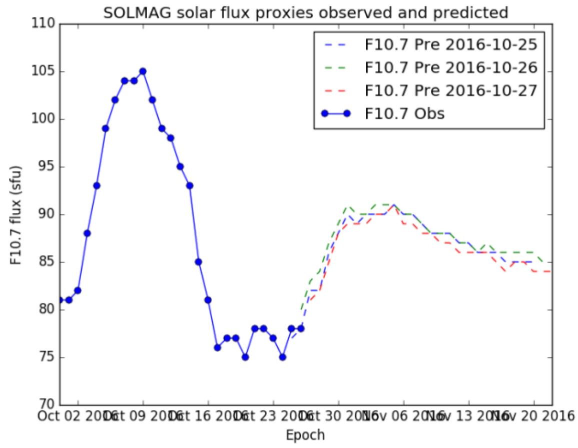

Figure 10. Observed solar flux F10.7 versus predicted flux at different epochs during the re-entry campaign.

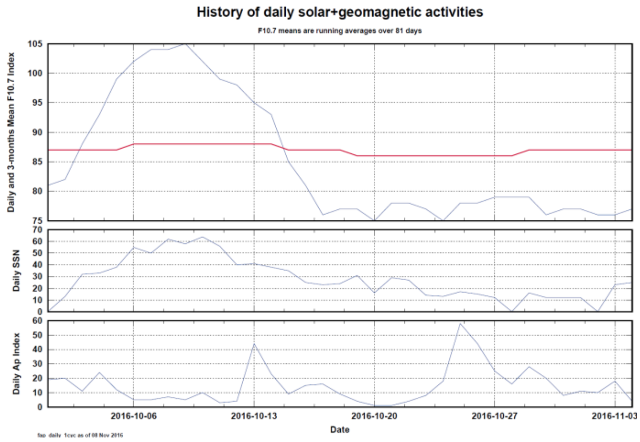

Figure 11. History of daily solar and geomagnetic activities for the last month before the AVUM re-entry.

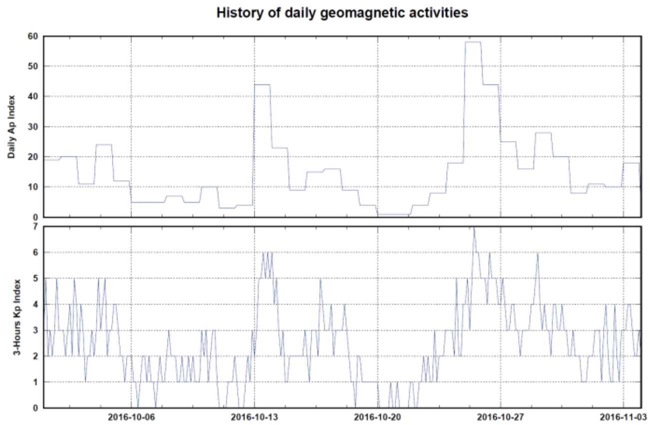

Figure 12. History of daily geomagnetic activities (Ap daily and Kp 3-hourly values) for the last month before the AVUM re-entry.

2.3 Atmosphere models

Different atmosphere models are implemented inside the suite of re-entry tools used at ESA Space Debris Office. It is known that the models, which have been generated using different data sources and are continuously being updated, have deficiencies, particularly at low altitudes and when the solar activity has extreme values (either high or low).

For the re-entry of the AVUM, the NRLMSIS-00 model [13] was used. As for the previous MSIS models, it accepts as input either a daily Ap value, or a combination of eight 3 hour Ap values. Although as default for re-entries we used only the daily Ap value, for this campaign we compared the results when using also the hourly Ap, in experimental mode. As the propagation uses the solar activity predictions, the only differences appear in the determination of the drag coefficient obtained from the fitting of various states. We observed that the residuals of the fitting were better when using the 3 hourly data at the beginning of the campaign and until the second solar storm (on the 29th of October), while afterwards the use of the daily Ap value provided slightly better results (as seen in Fig. 13 for the residuals in semi-major axis and in Fig. 14 for the residuals in true latitude). In all the cases, for the comparison we used the same time span for a single prediction using the different methods, but between different predictions it was varied to handle the solar activity variations. For the automated process, where always 20 US TLE are used for each prediction, the residuals were sometime smaller and other times larger than for the manual predictions. This could be explained by the use of different sources of orbital data in the manual predictions, which tend to be more noisy than using a single source.

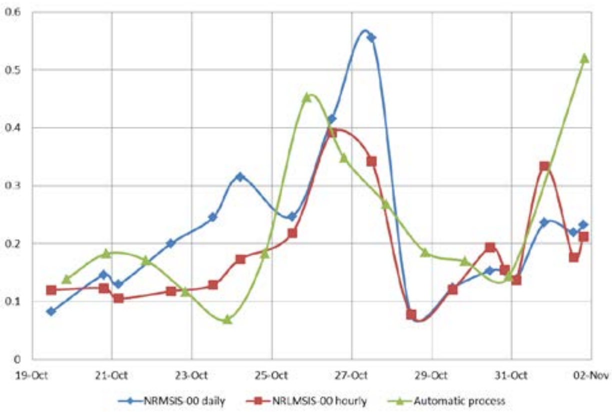

Figure 13. RMS in SMA (km) of the C_D fitting process.

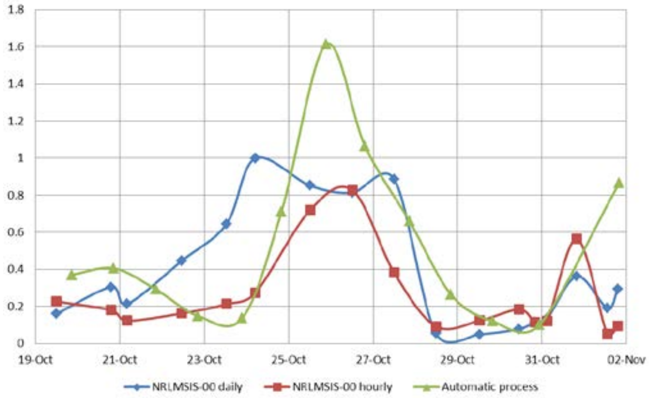

Figure 14. RMS in U (deg) of the CD fitting process.

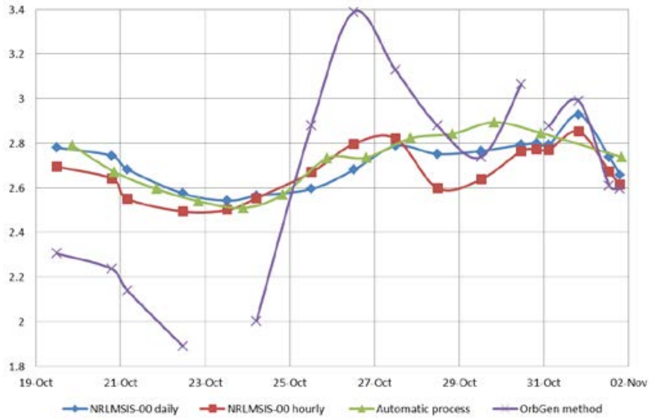

Figure 15. Cd evolution over the re-entry campaign using different computation method.

An alternative method to compute the drag coefficient was developed for this re-entry campaign. Instead of using a fast semi-analytical propagator (FOCUS (Fast Orbit Computation Utility Software)) in a single processor, this new method used an accurate numerical propagator (OrbGen) with parallel processing. The implementation estimates the ballistic coefficient BC, i.e. the product of area-to-mass ratio and drag coefficient, in an iterative process from a dataset of TLE. The first crude approximation is obtained by transforming the SGP4 B* coefficient. The coefficient is then improved using the last two TLEs of the dataset by minimizing the difference between the observed semi-major axis rate and the computed one. In order to safeguard the minimization process, the ballistic coefficient search is bounded to a feasible domain. Finally, the difference between observed and modelled semi-major axis for all selected TLEs is minimized using a linearly changing BC value.

In Fig. 15, we display the comparison of the obtained drag coefficients for the 17 re-entry predictions of the campaign, using the three different methods, as well as the daily automated process. As afterwards the three models used the same propagator and solar activity forecasts, the variation in drag coefficient correlates with a variation in the re-entry prediction time. The new method using the numerical propagator has the largest variation and seems very sensible to the solar activity, with peaks that can be correlated to the solar storms. This method uses also NRLMSIS-00 as atmosphere model and the daily Ap values, but other parameters in the force model are different, which explain some of the differences observed. In addition, some of the data points could not be computed with this technique. Further analysis and optimisation of this new developed method to estimate the BC is therefore required.

2.4 Predictions

The re-entry predictions were then made using the three different methods to compute the drag coefficient (with exactly the same data used for each of the predictions), plus automatically using only 20 US TLEs and with one prediction per day. The re-entry prediction times plus uncertainty margins are shown in Fig. 16 for the manual prediction using the default method (NRLMSIS-00 with daily Ap values), and in Fig. 17 for the automatic process.

As already said, to perform a manual prediction, many artifices are used to improve the results, as filtering out the wrong data, combining large amount of data from different sources, varying the length of the data span used for fitting in order to try to reduce the effects of the geomagnetic storms, combining noisy data to derive a mean state with less noise,… Thanks to all these improvements, we observe that the manual predictions have less variability than the automated ones, but they require still a lot of effort that has to be yet automatized. In Fig. 18, one can observe the many orbital states acquired during the campaign and how noisy they were.

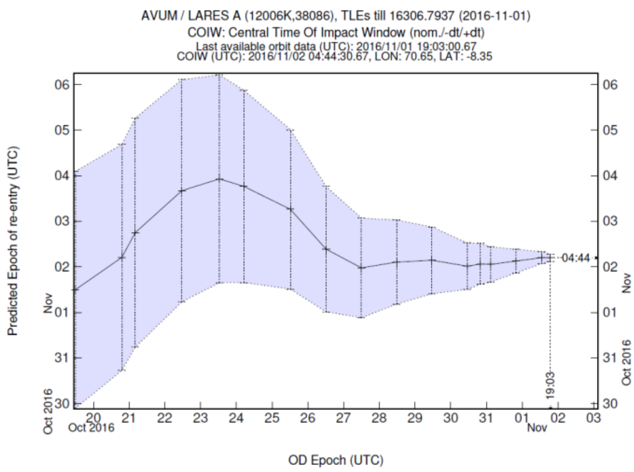

Figure 16. Re-entry prediction time and uncertainty margin for the AVUM re-entry campaign, issued from the manual processing.

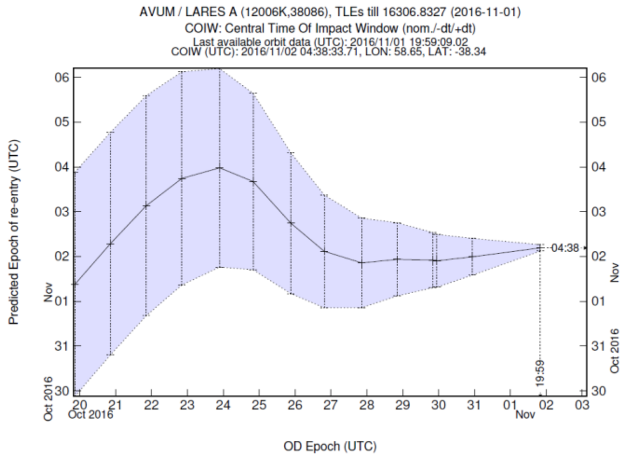

Figure 17. Re-entry prediction time and uncertainty margin for the AVUM re-entry campaign, issued from the automatic processing.

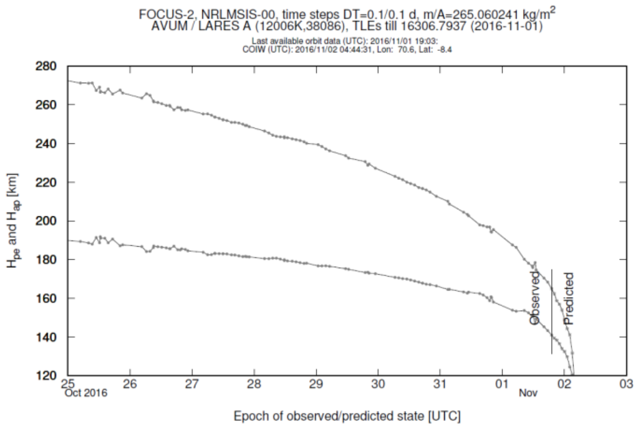

Figure 18. Apogee and perigee evolution of the observed states, and prediction for the remaining time, for the AVUM re-entry.

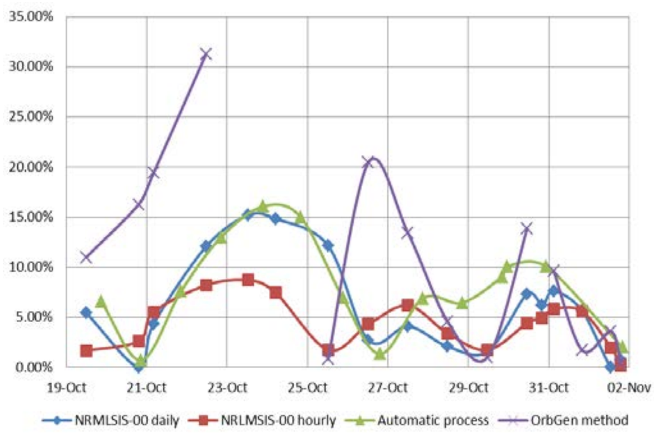

Figure 19. Relative errors of the predictions with different methods (as compared with the real re-entry time).

In any case, it is difficult to state which prediction method is better, because only the real re-entry time can be used as reference and it is only know after the re-entry, and the closer to the re-entry the better they converge. And it is possible that for some re-entry one method would work better, and for another a different one. A larger set of re-entries needs to be analysed with the different methods in order to assess it. Nonetheless, for the AVUM case, all of the methods used kept the real re-entry time inside the 20% uncertainty window (except of the new method based on OrbGen, for which further development is required), as can be seen in Fig. 19. Also, the manual predictions were in most of the cases better than the automatic process, especially in the last days of the campaign, and with the use of the 3-hourly Ap values, the error was always below 10%.

3 THE RE-ENTRY

3.1 Last prediction

The last prediction made by ESA used an orbital state at 19:03 UTC on the 1st of November 2017. With this data, the SDO predicted a re-entry of the AVUM at 4:44 UTC of the 2nd of November, with an uncertainty of ± 1.9 hours. This prediction excluded already some continents, but was very close to a decay over Asia, as can be seen in the ground track plot in Fig. 20.

In the last two weeks before the predicted re-entry, the SDO generates a series of plots and tables distributed to authorised users through the re-entry webpage [3], which are the re-entry time window evolution plot (Fig. 16), the perigee and apogee decay evolution (Fig. 18) and the ground track plot (Fig. 20) (which is also provided with the population density included). In the last days, extra plots are generated including risk figures (see Fig. 21), which take in account the predicted re-entry point and ground tracks, as well as the expected casualty area of the object (calculated either by accurate re-entry models as DRAMA or SCARAB, or using an approximation formula based on the mass of the object), and using the UN population distributions of the world, derive the risk to the population depending on the real re-entry time.

Figure 20. Ground track of the last prediction from ESA SDO including the uncertainty window.

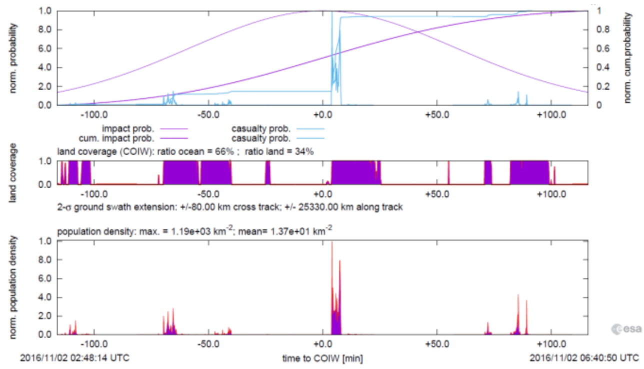

Figure 21. Risk figures for the last prediction of the AVUM re-entry.

Also in the last days, a table with the time that the object will spend above each of the countries is provided (Tab. 1), according to the ground track calculations.

Table 1. Time spent over each country according to the last prediction.

Country	Time Spent (s)
Ocean	9220
Russia	1660
United States	510
China	480
India	230
Canada	220
Argentina	180
Mongolia	180
Madagascar	180
Peru	180
Mexico	160
Chile	140
Kazakhstan	130
Afghanistan	110
Myanmar	60
Pakistan	60
Ecuador	50
Tajikistan	40
Kyrgyzstan	30
Nepal	30
Panama	20
Honduras	20
Thailand	20
Antarctica	20
Nicaragua	10
Fr. S. Antarctic Lands	10
Uzbekistan	10

3.2 Final re-entry

We received a confirmation by the US JSpOC saying that the object had re-entered, and that it had crossed the 80 km altitude threshold on the 2nd November 2016 at 4:43UTC, with an uncertainty window of 13 minutes. As for the IADC campaigns the re-entry point is provided at 10 km altitude, approximately 6 minutes have to be added to the above time, giving a re-entry at 4:49 UTC. The estimated impact ground track of the re-entry of AVUM based on the US time confirmation is provided in Fig. 22, and the central impact point is very close to the west coast of south India.

And in fact, two objects were found on ground, close to Karur and to Dindigul, in south India, which are both less than one minute further in the ground-track. Videos are available in YouTube on the recovery of these tanks by the local authorities, at *https://www.youtube.com/watch?v=FMnU_4_ihmY* and *https://www.youtube.com/watch?v=8DcBXYF-v28.*

The two objects seem to be tanks of the AVUM stage (displayed in Fig. 23). One is probably one of the four LPS propellant tank (Fig. 24) in the AVUM (two contain fuel and the other two the oxidizer). They are almost spherical shaped, made of titanium alloy and with a mass of 19.5 kg. The other object found is probably the LPS gas tank (Fig. 25), which is cylindrical shaped, made in an overwrapped configuration of carbon fiber and titanium liner, and with a mass of 21.5 kg. Both objects are now under custody of ISRO (Indian Space Research Organisation), and ESA is taking the required steps to bring the objects back to Europe in order to investigate the re-entry effects and be able to improve the re-entry models.

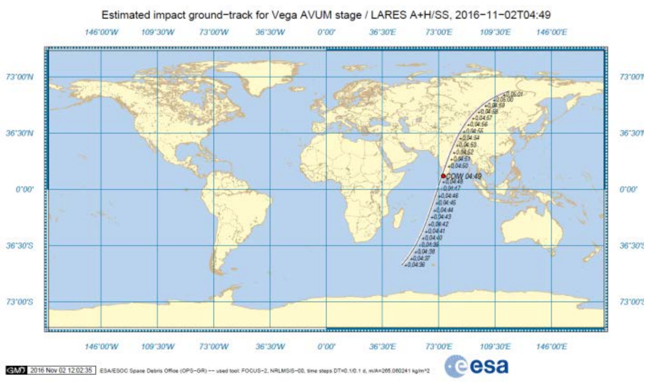

Figure 22. Estimated impact ground track.

Figure 23. Open view of the AVUM components and tanks.

Figure 24. Tank found close to Karur, India.

Figure 25. Tank found close to Dindigul, India.

4 CONCLUSION AND OUTLOOK

The re-entry of the VEGA-01 upper stage was followed with special interest in ESA (as ESA is the launching state for this object), and also in an internationally coordinated re-entry test campaign of the Inter-Agency Space Debris Coordination Committee (IADC).

For this re-entry campaign, the SDO handled data from many different sources and was able to integrate the data with success, improving the quality of the re-entry predictions.

Different methods were analysed in order to reduce the effects of the solar activity variability. One of the methods, using 3-hourly geomagnetic data instead of daily data, showed very promising results, with a reduced relative error compared to the other methods, and has now been implemented in the re-entry tools at the ESA SDO so that it can be automatically used in future re-entries. Another method using a numerical propagator instead of a semi-analytical one to compute the drag coefficient was developed, but the results were not to satisfactory and further analysis is required to understand the problems and address them.

At the end, the last predictions from ESA were very close to the real re-entry point, and it could be confirmed by two pieces found on ground, which did not cause any damage to people or property.

In order to further improve the re-entry process, for next campaigns we are going to continue developing and comparing the results using different atmosphere models and solar activity data inputs. In addition, we plan to compare the NRLMSIS-00 model with other models which are not yet implemented in the re-entry tools of the SDO (and could not be used for the AVUM campaign), as the DTM-2013 [14], which should be more accurate at lower altitudes, or the Russian GOST standard model, in order to determine which model behaves better in re-entry conditions.

5 REFERENCES

1. Bunte, K. D., Sdunnus, H., Mandeville, J.C., & Klinkrad, H. (2001). Ballistic Parameter and Lifetime Assessment for Catalogued Objects. In *Proceedings of the 3th European Conference on Space Debris*, ESA, Darmstadt, Germany.

2. Flohrer, T., et al. (2013). DISCOS: Current Status and Further Developments. In *Proceedings of the 6th European Conference on Space Debris,* ESA, Darmstadt, Germany.

3. ESA's re-entry predictions. Online at: *https://reentry.esoc.esa.int/*

4. Lemmens, S., Bastida Virgili, B. et al. (2016). From End-Of-Life To Impact On Ground: An Overview Of Esa's Tools And Techniques To Predicted Re-Entries From The Operational Orbit Down To The Earth's Surface. In *Proceedings of the 6th ICATT,* ESA, Darmstadt, Germany.

5. Vega first launch. Online at: *http://www.esa.int/Our_Activities/Launchers/Launch_vehicles/Vega_first_launch/Flight_overview*

6. Inter-Agency Space Debris Coordination Committee. (2002). IADC Space Debris Mitigation Guidelines. IADC-02-01.

7. Alarcón-Rodriguez, J. R., Klinkrad, H., Cuesta J. & Martinez, F. M. (2005). Independent Orbit Determination for Collision Avoidance. In *Proceedings of the 4th European Conference on Space Debris*. ESA SP-587.

8. EISCAT scientific association. Online at: *https://www.eiscat.se/*

9. Mugellesi-Dow, R., Kerridge, D. et al. (1993) SOLMAG: an operational system for prediction of solar and geomagnetic indices. In *Proceedings of the 1st European Conference on Space Debris.*

10. McNish, A. & Lincoln, J. (1949). Predictions of sunspot numbers. *Trans.Am.Geophys.Union*. **30**, 673-685.

11. Holland, R. & Vaughan, W. (1984) Lagrangian least-squares prediction of solar flux (F10.7). *J.Geophys. Res.*, **89**, No. A1, 11-16.

12. SIDC – Solar Influence Data Analysis Center. Ursigram. Online at: *http://sidc.oma.be/products/meu/*

13. Picone, J. M., Hedin, A. E., Drob, D. P., Aikin, A. C. (2002). NRLMSISE-00 empirical model of the atmosphere: Statistical comparisons and scientific issues. *Journal of Geophysical Research: Space Physics.* **107** (A12): 1468.

14. Bruinsma, S. (2015) The DTM-2013 thermosphere model. *Journal of Space Weather and Space Climate*, **5**, id.A1, 8 pp.